Tillman *et al.*
Journal of NeuroEngineering and Rehabilitation (2024) 21:145
https://doi.org/10.1186/s12984-024-01437-3

Journal of NeuroEngineering and Rehabilitation

RESEARCH

Open Access

Healthy older adults generate transverse-plane momenta required for 90° turns while walking during the same phases of gait as used in straight-line gait

Mitchell Tillman[1], Jun Ming Liu[1], Zahava M. Hirsch[1], Janine Molino[2,3] and Antonia M. Zaferiou[1*]

Abstract

Background Generation and regulation (control) of linear and angular momentum is a challenge during turning while walking which may be exacerbated by age-related changes. In healthy older adults, little is known about how momentum is controlled during turns, especially within each phase of gait. Each phase of gait affords unique mechanical contexts to control momenta and regulate balance. In healthy young adults, we found that the transverse-plane linear and angular momenta generation strategies observed within specific phases of gait during straight-line gait were also used during turns. Therefore, in this study, we investigated whether healthy older adults shared similar momentum control strategies specific to each gait phase during straight-line gait and turns.

Methods Nine healthy older adults completed straight-line gait and 90° leftward walking turns. We compared the change in transverse-plane whole-body linear and angular momentum across gait phases (left and right single and double support). We also compared the average leftward force and transverse-plane moment across gait phases.

Results We found that leftward linear momentum was generated most during right single support in straight-line gait and leftward turns. However, in contrast to straight-line gait, during leftward turns, average leftward force was applied across gait phases, with left single support generating significantly less leftward average force than other gait phases. Leftward angular momentum generation and average moment were greatest during left double support in both tasks. We observed some within-participant results that diverged from the group statistical findings, illustrating that although they are common, these momenta control strategies are not necessary.

Conclusions Older adults generated transverse-plane linear and angular momentum during consistent phases of gait during straight-line gait and 90° turns, potentially indicating a shared control strategy. Understanding momentum control within each phase of gait can help design more specific targets in gait and balance training interventions.

Keywords Motor control, Biomechanics, Momentum, Gait, Turn, Rotation, Older adults, Locomotion

*Correspondence:
Antonia M. Zaferiou
Antonia.Zaferiou@stevens.edu
[1] Department of Biomedical Engineering, Stevens Institute of Technology, Castle Point on the Hudson, Hoboken, NJ 07030, USA
[2] Department of Orthopaedics, Warren Alpert Medical School of Brown University/Rhode Island Hospital, Providence, RI, USA
[3] Lifespan Biostatistics, Epidemiology, and Research Design Core, Rhode Island Hospital, Providence, RI, USA

Introduction

Linear and angular momentum must be generated and regulated (i.e., controlled) in the transverse plane to walk in a straight-line and to navigate real-world environments that require turning while walking. To walk in daily life, these momenta must be controlled through multilayered sub-system controller actions (e.g., muscle torques, etc.) so that the destination is reached without a fall [1]. Notably, up to 50% of our daily steps are part of turning gait, depending on the environment [2], and turning challenges momenta control beyond the demands of straight-line gait [3]. In older adults, turns are more difficult to execute due to age-related physiological changes which affect momenta control, even in healthy older adults, such as declines in muscle strength and coordination [4].

Prior research has described linear and angular momentum patterns during straight-line gait in healthy young and older adults towards quantifying balance. In straight-line gait, linear momentum exhibits small oscillations about zero in the medial–lateral (ML) direction [5] as weight shifts from one footfall to the next. Other work has shown that angular momentum during straight-line gait is maintained near zero, oscillating about zero in each plane over the course of the gait cycle [1]. Coordinating linear and angular momenta in straight-line gait allows maintenance of a constant speed and direction while facilitating balance. In turns, less is known about the neuromechanics of momenta control.

In walking turns, transverse-plane linear and angular momentum must be redirected towards the new direction of travel [6]. Specifically, linear momentum must be generated in the new desired direction travel so that the center of mass (COM) trajectory can redirect. In the angular domain, angular momentum must be generated to rotate the body about a vertical axis passing through the COM to change the body's facing direction. While there are few prior studies about how older adults' momentum is controlled during turns, in young and middle aged healthy adults, transverse-plane linear momentum redirection has been shown to occur via medially directed forces over the course of the "outside" foot's stance phase (e.g., right leg stance phase during leftward turn) [7–9]. During turns, transverse-plane angular momentum diverges from oscillating about zero [3] in order to achieve body rotation about vertical. For example, during a 90° turn, average transverse-plane angular momentum was greater than it was during straight-line gait [10].

Investigating momentum generation within each of the four phases of gait is helpful because each gait phase affords unique mechanical contexts and turning while walking can occur over multiple steps [2]. This detailed information can be used in future rehabilitative practices to help diagnose motor control disfunction and train momenta generation strategies specific to base of support contexts. For example, if axial body rotation and balance are facilitated when both legs are in contact with the ground, gait retraining approaches can provide more specific body rotation targets for double support gait phases. Using a framework to investigate the contribution of each gait phase to momenta control, in young adults we found indicators of momenta control strategies that were specific to each gait phase during seemingly disparate tasks [6]. Specifically, during straight-line gait, pre-planned and late-cued 90° leftward turns, leftward transverse-plane linear and angular momentum were primarily generated during right single support and left double support phases, respectively The mechanical context to generate linear and angular impulses differs greatly as the COM and base of support relationship changes between single and double support phases in bipedal locomotion. Thus, our previous findings in young adults suggest that they leverage transverse-plane linear and angular momenta control specific to the gait phases during both straight-line gait and walking turns, despite differences in momenta control demands and footfall patterns across these tasks [6].

The primary purpose of this study was to understand whether transverse-plane linear and angular momentum generation in older adults occurs during the same phases of gait in straight-line gait and 90° turns. We hypothesized that both the straight-line gait and 90° left turn tasks will exhibit (1) the largest increase in linear momentum (Δp_x) and average leftward force ($F_{x,avg}$) towards the new direction of travel during right single support vs. other gait phases, and (2) the largest leftward change in transverse-plane angular momentum (ΔH_z) and average moment ($M_{z,avg}$) during left double support vs. other gait phases.

Methods

Participants

Nine older adults (2 male, 7 female; 71 ± 6 years; 73.6 ± 15.4 kg; 1.65 ± 0.06 m) participated in this experiment after providing informed consent per Stevens Institute of Technology Institutional Review Board requirements. To meet the inclusion criteria, participants were over the age of 65 and indicated that they had not fallen within the prior six months, could walk at least one fourth of a mile unassisted in the community, scored 23 or higher on the Montreal Cognitive Assessment [11] and 19 or higher on the Dynamic Gait Index [12] (see Supplemental Document 1 for participant scores) and were free of injury or pain in the lower extremities.

Experiment setup and protocol

Twenty optical motion capture cameras tracked participants' movements at 250 frames per second (Optitrack, Corvallis, OR USA). Rigid tracking marker clusters each with four reflective markers were affixed via athletic wrap to the following segments: left and right foot, shank, thigh, forearm, and upper arm. To track the torso, a chest harness with four markers was worn; and to track the head, a headband with four markers was worn above the ears. To track the pelvis, four individual markers were adhered to each of the left and right anterior and posterior superior iliac spines. The mappings from tracking markers to anatomic markers were established during calibration trials using a pointing device (Probe Kit, Optitrack, Corvallis, OR). Previously established methods were used to compute hip joint centers [13] and shoulder joint centers [14]. The full-body biomechanical model was then constructed following the method from Dumas et al. [15].

Similar to methods we previously described in a study of young adults [6], bright blue tape was placed on the black floor to form a walkway in the shape of a T-intersection (Fig. 1). Additional brightly colored plastic vertical poles were placed at the corners of the intersection extruding upward from plastic cones so that the participants had an additional visual cue of the intersection to avoid excessive visual gaze to the floor to see the tape. These poles also may have limited inward lean at the intersection to avoid contact with the poles [16]. The walkway was 0.91 m (36 inches) wide, per ADA requirements [17]. The + Y direction was 10 m long, with the intersection halfway down the walkway, and the − X direction was 4 m long.

A licensed physical therapist was present to perform standard gait assessments and to guard the participants' balance during every trial. During a prior lab visit, the participants were screened to ensure they met the inclusion criteria. At the beginning of the data collection lab visit, the physical therapist ensured participants were alert and oriented, measured their vitals (e.g., heart rate, blood pressure, respiratory rate, etc.), visual analog pain scale scores, and visual analog perceived rate of exertion. Then, the physical therapist performed manual muscle testing for each degree of freedom for the hip, knee, and ankle, along with a foot sensation 10 g monofilament test [18] and a proprioceptive contralateral joint matching test. Finally, participants performed the miniBEST test [19]. These data are provided in Supplemental Document 1.

After calibration tasks and baseline assessments, participants performed two tasks in sequential order. First, in the straight-line gait task, they walked within a 10 m walkway at their comfortable pace. In the turning task, they walked 5 m within the walkway, turned 90° to the left at an intersection, and walked 4 m in the new direction before stopping. Each task was repeated 12 times after two to four practice trials. Participants were also instructed on which foot to begin walking with, randomized such that 50% of trials began with the left foot, like methods previously described [6].

Data analyses

Data analyses were conducted in MATLAB (Mathworks, Natick, MA). Data were smoothed and gap-filled (MATLAB's 'csaps' function with smoothing parameter set to 0.0005). One trial each from two participants were excluded due to reflective marker occlusion issues. The full-body biomechanical model [15] was computed using the relationship between each segment's rigid tracking marker clusters and anatomic landmark positions, which also provided each segment's mass and tensor of inertia. During the straight-line gait and turning tasks, linear momentum of the center of mass in the lab X direction (Fig. 1) and angular momentum about the vertical axis through the center of mass were computed at each frame, as previously described [6].

Linear momentum and angular momentum

Linear momentum $\vec{p}$ was computed in the lab's fixed reference frame. Scalar p_x and p_y are the components along the lab's fixed X and Y axes.

Angular momentum $\vec{H}$ about the COM was computed using the formula from ref. [1]. The $\vec{H}$ vector is then expressed in a reference frame aligned with the pelvis to approximate the frontal-plane of the body [15], where + x points from left to right anterior superior iliac spine in the horizontal plane, + z is the lab's vertical axis, and + y is in the horizontal plane perpendicular to + x and + z following the right-hand rule. Scalar frontal (H_f) and transverse (H_z) plane angular momentum values were obtained by extracting the second and third components of $\vec{H}$, respectively.

Phase of interest

During straight-line gait, the phase of interest was the middle ~ 4 m of the walkway, bounded by heel strike events. The turn phase was defined by when pelvis heading (yaw) angle exceeded a threshold value, as described in ref. [6] (Fig. 1C). This threshold was defined during straight-line gait as three times the standard deviation of the pelvis heading. During turning trials, when the pelvis heading angle exceeded this threshold value relative to the + Y lab axis, the turn phase was determined to start. The turn phase end was determined by when the pelvis heading angle relative to the − X lab axis decreased below the threshold value. The turn phase start and end

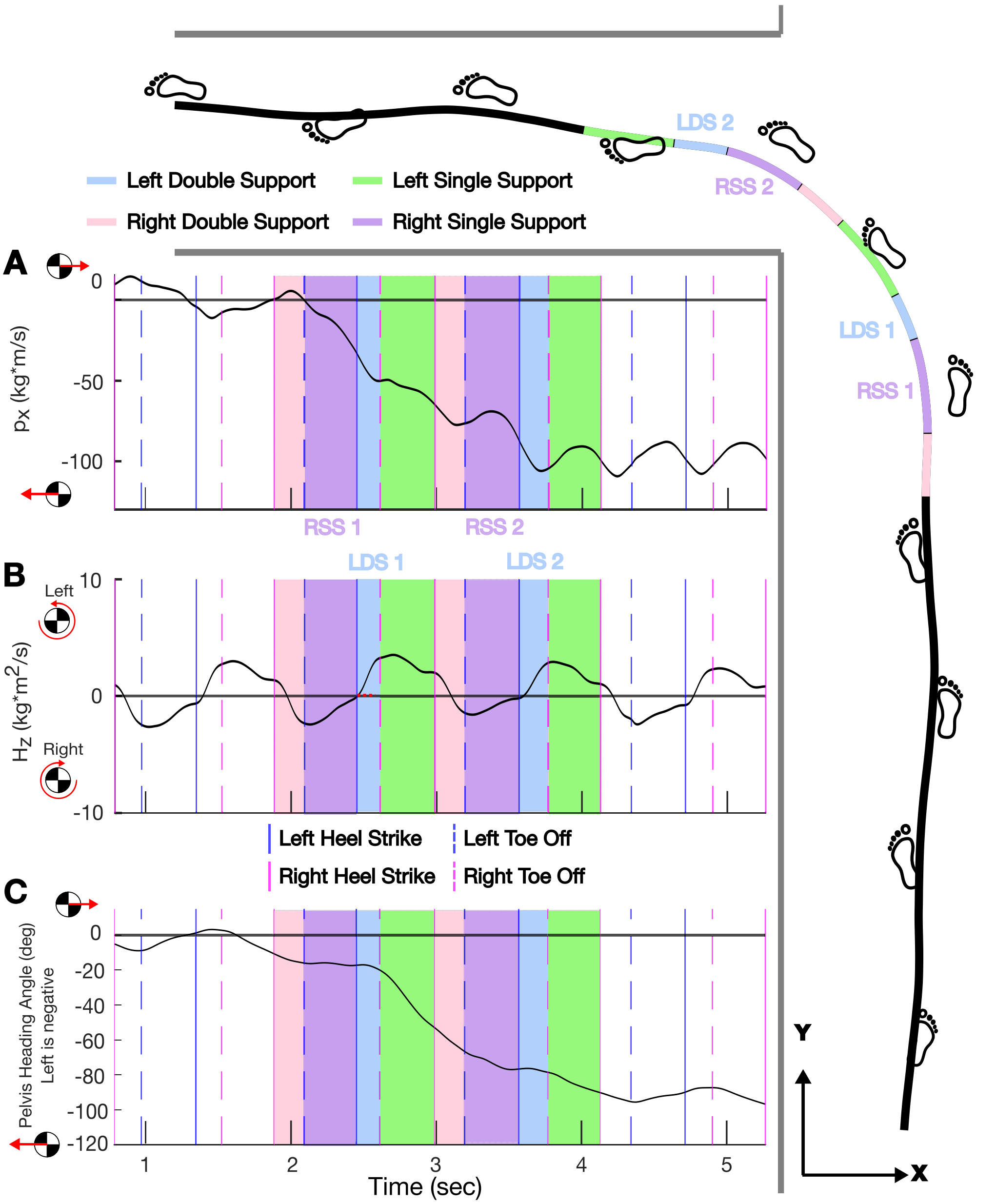

Fig. 1 Example timeseries and COM trajectory during a 90° turn trial (participant 6). The footfall locations (at mid-stance) and COM trajectory—colored black before and after the turn phase, colored by gait phase within the turn phase. On the timeseries graphs (**A**–**C**), gait phases during the turn are color coded

were then extended backwards and forwards in time, respectively, to the nearest heel strike event to ensure consistency in base of support context during the turn phase across trials [6, 20].

Gait phase computations

Gait events were computed using the method from Zeni et al. [21] adapted for turning gait [22]. Left and right single and double support phases are the intervals between the corresponding gait phases. For example, left double support is the interval between left heel strike and right toe off.

The change in linear momentum (Δp) and angular momentum (ΔH) within each gait phase was computed as the final minus initial value during each phase. Then, average force (F_{avg}) and moment (M_{avg}) were computed by dividing Δp and ΔH by each phase's duration (in seconds).

When more than one repetition of a gait phase occurred during a turn, (e.g., two right single support phases in Fig. 1), their values were averaged. Thus, for each metric we obtained one value per trial for each of the four gait phases.

Contextual descriptive measures

In addition to the metrics in our hypotheses, we also computed descriptive measures, such as horizontal walking speed ($\left|\vec{v}_{horiz}\right|$) and turn strategy to explore potential moderating variables. Turn strategy was computed following the method from ref. [23]. To provide additional context of our findings when discussing results, we computed lateral distance (LD), which is the horizontal distance from the center of mass to the nearest lateral edge of the base of support, in the direction aligned with the pelvis-fixed mediolateral axis [20]. These additional measures' data are included in Supplemental Document 1 for future reference and results tables and results figures are in Supplemental Document 3 to provide context within the discussion.

Statistical analyses

A linear mixed model was used to account for the hierarchical relationships of the data. Fixed effects (main factors) included gait phase, task, and a gait phase by task interaction. Additionally, there were random intercepts for study participant and random slopes for trial number nested within task and participant (*proc glimmix* in SAS version 9.4; SAS Institute Inc., Cary, NC). Pairwise comparisons between gait phases within task and between task within gait phase were conducted within the model via orthogonal contrasts. The Holm test was used to adjust for multiple comparisons, maintain a two-tailed familywise alpha of 0.05 across all comparisons. We also performed two secondary analyses to preliminarily explore whether turn strategy ("spin" vs. "step" turns [24]) or gait speed, respectively, moderated the relationship between gait phase and outcome measures for each task (Supplemental Document 2). This study quantifies "step turns" as those with the outside foot placement closest to the center of the intersection (i.e., right foot during leftward turn) and "spin turns" with the inside foot placement closest to the center of the intersection (i.e., left foot during leftward turns) [6, 20, 23].

Results

Data to reproduce these results are provided in Supplemental Document 1.

Global leftward (−X) change in linear momentum (Δp_x) and average force ($F_{x,avg}$).

The largest Δp_x in the -X direction occurred during right single support phase during straight-line gait ($p < 0.0001$, Table 1) and turns ($p \leq 0.02$). $F_{x,avg}$ was largest in the -X direction during right single support phase only during straight-line gait ($p \leq 0.0006$). During turns, left single support $F_{x,avg}$ was significantly smaller than all other gait phases ($p \leq 0.0009$), while the other gait phases were not significantly different from one another ($p \geq 0.11$). Within-participant data is shown in Figs. 2 and 3 and within-participant statistical analyses are included in Supplemental Document 4.

Transverse-plane change in angular momentum (ΔH_z) and average moment ($M_{z,avg}$)

ΔH_z leftward was largest during left double support phase during each straight-line gait ($p \leq 0.009$, Table 1) and turns ($p \leq 0.005$). $M_{z,avg}$ was also largest during left double support during straight-line gait ($p < 0.0001$) and turns ($p < 0.0001$). Within-participant data is shown in Figs. 4, 5 and within-participant statistical analyses are included in Supplemental Document 4.

Between-task comparison of primary variables within gait phase

Δp_x and $F_{x,avg}$ both differed in straight-line gait vs. turns for all gait phases ($p \leq 0.009$, Table 1). ΔH_z and $M_{z,avg}$ both did not differ between straight-line gait and turns for any gait phase ($p = 0.99$; Table 1).

Additional contextual measures

While there were no hypotheses for auxiliary measures, they are included in Supplemental Document 3 to provide additional context. LD_{min} during straight-line gait was not different between any gait phase except that LD_{min} during left double support was less than during right single support ($p = 0.02$). During leftward turns, the LD_{min} occurred during left single and double support (p-values left single or left double support vs. all other gait phases < 0.0001). $H_{f,min}$ was most negative (i.e., body above the COM rotates leftward) during left double support and right single support (compared to all other gait-phases, $p \leq 0.0014$) during straight-line gait. During turns, all gait phases' $H_{f,min}$ besides right double support were not different ($p \geq 0.09$).

Discussion

The purpose of this study was to investigate how whole-body transverse-plane linear and angular momentum are generated within each phase of gait to execute straight-line gait and 90° pre-planned left turns. This

Table 1 Group-level estimated marginal means (95% confidence interval) and p-values of comparisons of linear and angular momentum variables across gait phase and across task

	Task	Estimated Marginal Mean (95% CI)				Post-hoc comparisons (p-value)					
		LDS	LSS	RDS	RSS	LDS v. LSS	LDS v. RDS	LDS v. RSS	LSS v. RDS	LSS v. RSS	RDS v. RSS
Δp_x (kg+m/s)	Straight-line gait (S)	− 1.95 (− 2.86, − 1.04)	10.05 (8.55, 11.55)	1.70 (0.45, 2.96)	− 9.71 (− 12.04, − 7.38)	**< 0.0001**	**< 0.0001**	**< 0.0001**	**< 0.0001**	**< 0.0001**	**< 0.0001**
	Pre-planned turns (PP)	− 11.64 (− 13.45, − 9.83)	− 6.24 (− 9.30, − 3.17)	− 8.32 (− 10.10, − 6.55)	− 18.76 (− 22.81, − 14.72)	**0.01**	**0.02**	**0.008**	0.24	**< 0.0001**	**< 0.0001**
	S vs. PP (p-value)	**< 0.0001**	**< 0.0001**	**< 0.0001**	**0.001**	–	–	–	–	–	–
$F_{x,avg}$ (kg+m/s^2)	Straight-line gait (S)	− 10.45 (− 15.14, − 5.78)	28.08 (23.46, 32.69)	8.78 (2.61, 14.96)	− 26.99 (− 33.47, − 20.50)	**< 0.0001**	**< 0.0001**	**0.0006**	**< 0.0001**	**< 0.0001**	**< 0.0001**
	Pre-planned turns (PP)	− 60.83 (− 71.17, − 50.48)	− 16.17 (− 24.23, − 8.11)	− 44.20 (− 55.75, − 32.64)	− 50.37 (− 60.27, − 40.47)	**< 0.0001**	0.11	0.30	**0.0009**	**< 0.0001**	0.42
	S vs. PP (p-value)	**< 0.0001**	**< 0.0001**	**< 0.0001**	**0.0009**	–	–	–	–	–	–
ΔH_z (kg+m^2/s)	Straight-line gait (S)	2.57 (2.02, 3.12)	− 1.38 (− 1.81, − 0.94)	− 2.62 (− 3.11, − 2.14)	1.43 (1.01, 1.85)	**< 0.0001**	**< 0.0001**	**0.009**	**0.002**	**< 0.0001**	**< 0.0001**
	Pre-planned turns (PP)	2.55 (2.07, 3.03)	− 1.31 (− 1.65, − 0.98)	− 2.59 (− 3.11, − 2.06)	1.36 (0.88, 1.84)	**< 0.0001**	**< 0.0001**	**0.005**	**0.001**	**< 0.0001**	**< 0.0001**
	S vs. PP (p-value)	0.99	0.99	0.99	0.99	–	–	–	–	–	–
$M_{z,avg}$ (kg+m^2/s^2)	Straight-line gait (S)	14.13 (11.27, 17.00)	− 3.85 (− 5.09, − 2.60)	− 14.55 (− 17.04, − 12.06)	4.02 (2.79, 5.26)	**< 0.0001**	**< 0.0001**	**< 0.0001**	**< 0.0001**	**< 0.0001**	**< 0.0001**
	Pre-planned turns (PP)	13.39 (10.85, 15.93)	− 3.52 (− 4.43, − 2.60)	− 13.27 (− 15.34, − 11.19)	3.73 (2.41, 5.04)	**< 0.0001**	**< 0.0001**	**< 0.0001**	**< 0.0001**	**< 0.0001**	**< 0.0001**
	S vs. PP (p-value)	0.99	0.99	0.99	0.99	–	–	–	–	–	–

Bolded p-values indicate statistically significant differences

LDS: Left Double Support; LSS: Left Single Support; RDS: Right Double Support; RSS: Right Single Support; Δp_x: change in global X-axis linear momentum; $F_{x,avg}$: global X-axis average force, where negative X is leftward (the direction of the turn); ΔH_z: change in transverse-plane angular momentum; $M_{z,avg}$: average transverse-plane moment, where positive is leftward

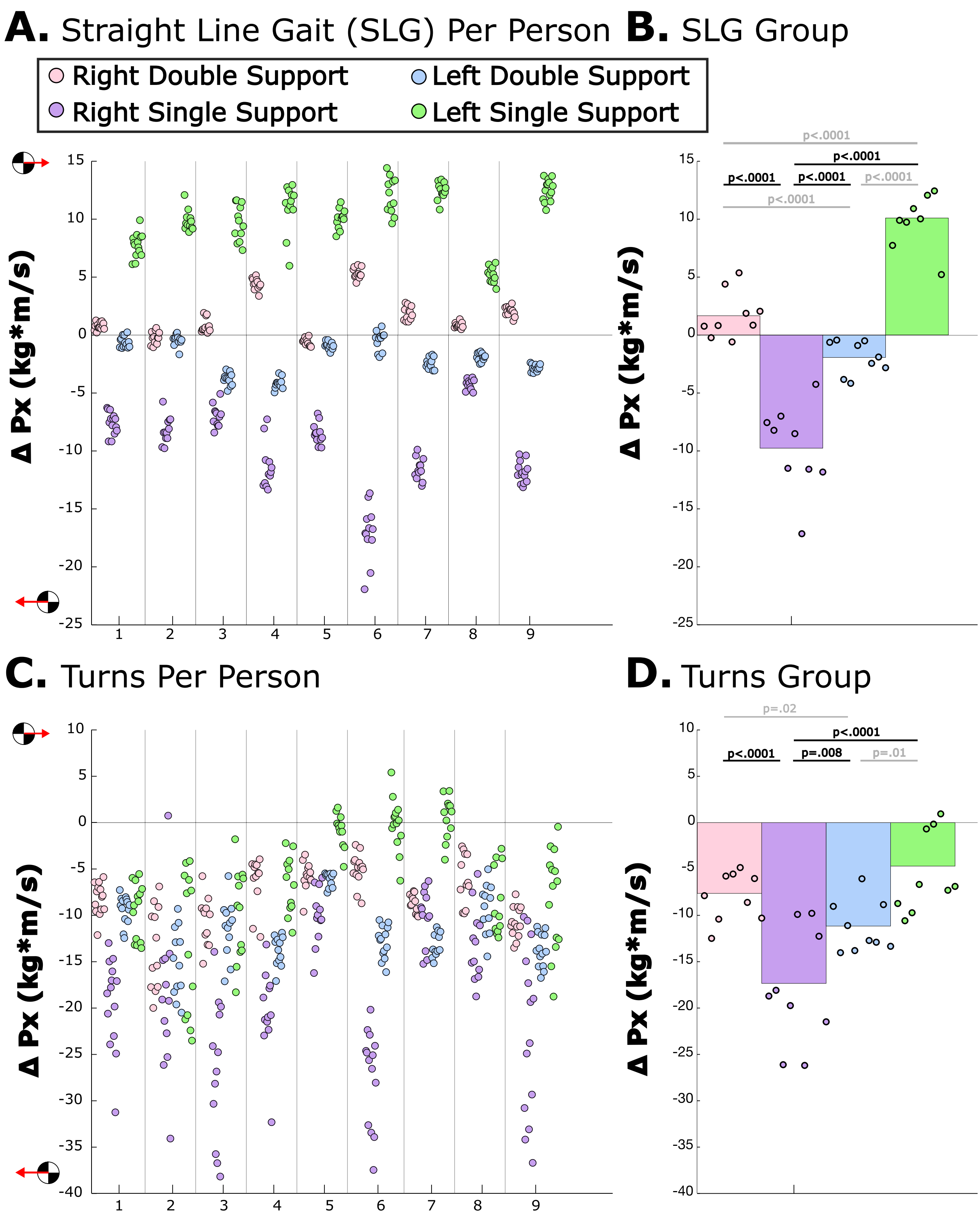

Fig. 2 The change in global X-axis linear momentum (Δp_x) for each gait phase during **A**, **B** straight-line gait, and **C**, **D** turns. Negative p_x is leftward in the direction of the turn. The left panel **A**, **C** provides average Δp_x for each gait phase, each trial, and each participant. In the right panel **B**, **D**, each circle indicates the average value for each participant across multiple trials and the bar represents the across-participant (group) averages. Horizontal lines with p-values indicate statistically significant differences between gait phases at the group level, those in gray are significant differences that were not related to the hypotheses

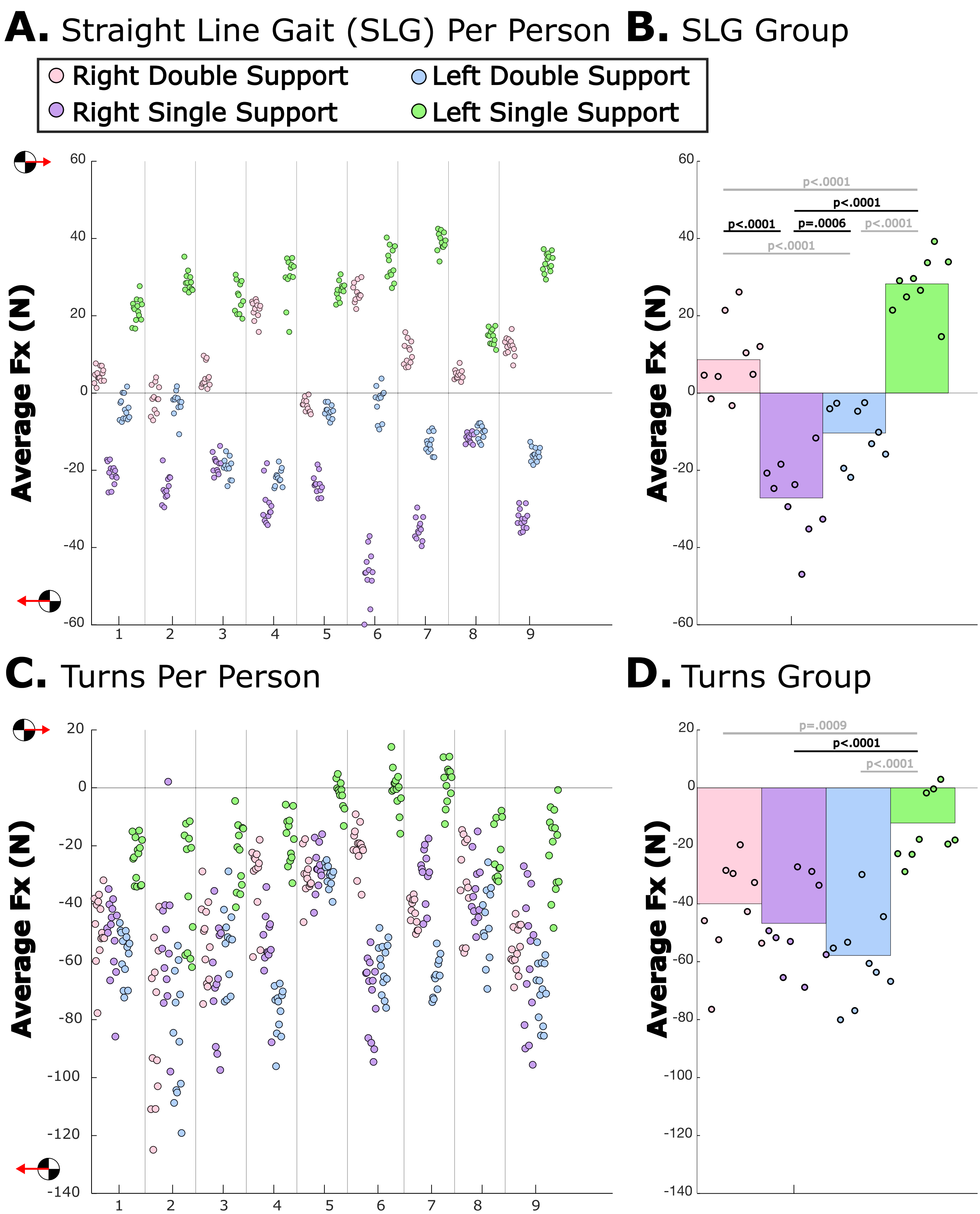

Fig. 3 The average global X-axis force ($F_{x,avg}$) for each gait phase during **A**, **B** straight-line gait, and **C**, **D** turns. Negative $F_{x,avg}$ is leftward in the direction of the turn. The left panel **A**, **C** provides average $F_{x,avg}$ for each gait phase, each trial, and each participant. In the right panel **B**, **D**, each circle indicates the average value for each participant across multiple trials and the bar represents the across-participant (group) averages. Horizontal lines with p-values indicate statistically significant differences between gait phases at the group level, those in gray are significant differences that were not related to the hypotheses

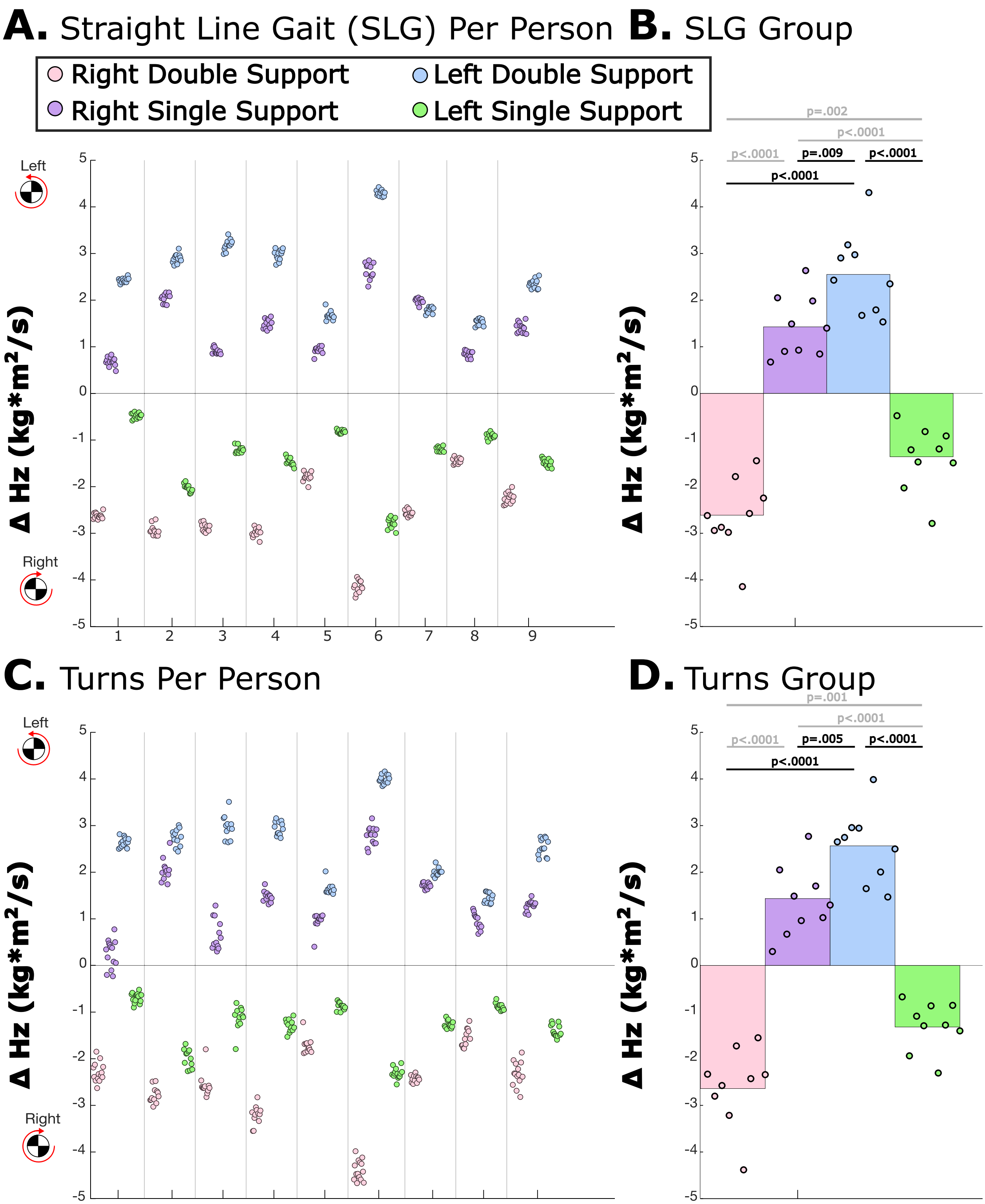

Fig. 4 The change in transverse-plane angular momentum (ΔH_z) for each gait phase during **A**, **B** straight-line gait, and **C**, **D** turns. Positive ΔH_z is leftward in the direction of the turn. The left panel **A**, **C** provides average ΔH_z for each gait phase, each trial, and each participant. In the right panel **B**, **D**, each circle indicates the average value for each participant across multiple trials and the bar represents the across-participant (group) averages. Horizontal lines with p-values indicate statistically significant differences between gait phases at the group level, those in gray are significant differences that were not related to the hypotheses

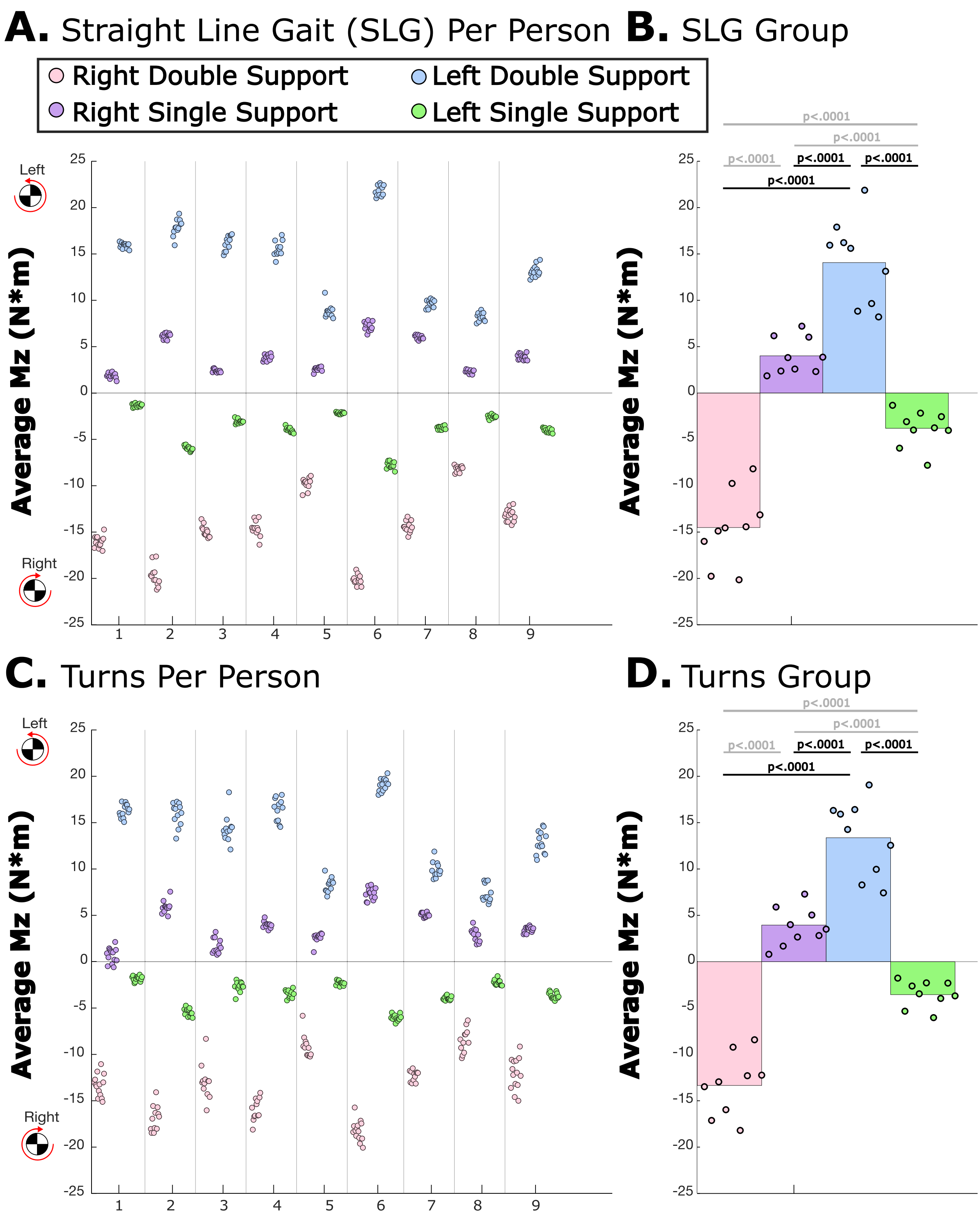

Fig. 5 The average transverse-plane moment about a vertical axis through the COM ($M_{z,avg}$) for each gait phase during **A**, **B** straight-line gait, and **C**, **D** turns. Positive $M_{z,avg}$ is leftward in the direction of the turn. The left panel **A**, **C** provides average $M_{z,avg}$ for each gait phase, each trial, and each. In the right panel **B**, **D**, each circle indicates the average value for each participant across multiple trials and the bar represents the across-participant (group) averages. Horizontal lines with p-values indicate statistically significant differences between gait phases at the group level, those in gray are significant differences that were not related to the hypotheses

purpose aims to inform more specific targets for future clinical interventions. Our first hypothesis, that leftward linear momentum would be generated most during right single support in straight-line gait and turns, was supported for Δp_x in both tasks. For $F_{x,avg}$, this was only supported during straight-line gait: during turns, right single support was not different from any gait phase besides left single support, with left single support generating the least average leftward force. We also hypothesized that leftward transverse-plane angular momentum about the center of mass would be generated most during left double support, which was supported for both ΔH_z and $M_{z,avg}$. These results suggest that during both straight-line gait and turns, a common control strategy is used to generate COM leftward linear momentum during right single support phase and changes in body-facing direction leftward are initiated most during the left double support phase of gait. This similarity occurred despite a variety of footfalls used to perform the turns (data in Supplemental Document 1; example trials provided in Fig. 1 and Supplemental Fig. 3.1).

This older adult cohort generated leftward linear momentum primarily during right single support. In straight-line gait, the body shifts weight between left and right feet, with the largest mediolateral accelerations during the single support phases [5]. When focusing on leftward weight shifts in straight-line gait, the right single support phase facilitates the largest leftward linear momentum generation because it allows the COM to travel leftward leading to the left foot's heel strike. Thus, the body progresses to the left foot and the left double support phase can arrest leftward linear momentum in order for the COM to remain within the base of support. The other gait phases do not facilitate the ability to accelerate the COM leftward without imposing a greater challenge to medial–lateral balance maintenance. For example, during right single support, if excess leftward linear momentum is generated, this excess momentum can be controlled by placing the left foot more laterally than normal. In contrast, if excess leftward linear momentum is generated during left single support, a cross-over step may be needed, and is more challenging to coordinate [5, 25]. When completing a walking turn, the affordances of these gait phases remain similar for generating the greatest linear momentum leftward during right single support. However, there were differences in how much each gait phase contributes to leftward forces between straight-line gait and pre-planned 90° leftward turns.

During pre-planned 90° leftward turns, all gait phases generated leftward linear momentum and average leftward force, with significantly less average leftward force generated during left single support. This result was also exhibited by young adults in our previous study [6], though future studies can directly compare across young and older adult cohorts. This is sensible because if the left single support gait context is when people generate leftward forces similar to those generated during other gait phases, excess lateral momentum could conflict with balance maintenance (as discussed in the previous paragraph). Using multiple gait phases to generate linear momentum and average force in the new direction of travel is beneficial during turns, given the increased demand to do so relative to the demand during straight-line gait.

This older adult cohort generated the greatest leftward angular momentum and average moment (ΔH_z and $M_{z,avg}$) during left double support. This finding was also observed in young adults [6], though future studies can directly compare across cohorts. In straight-line gait, the body oscillates in small, approximately symmetric, rotations about vertical [1]. Specifically, during left double support, the body starts to rotate to the left to prepare for the right leg to push off the ground (the zero-crossings are at heel strikes) [6]. Left double support phase facilitates the largest leftward change in angular momentum and average moment because double support enables greater control of body rotation without compromising balance. This is because extraneous linear impulses can be concurrently neutralized by both support legs [6, 26]. Finally, there were no significant differences in angular momentum and moment generation between tasks, within each gait phase. This indicates that, unlike linear momentum, angular momentum generation patterns were consistent between straight-line gait and turns. Although the demand to rotate the body to a new facing direction increases in turns vs. straight-line gait, the gait phase contributions to rotating the body about vertical remain similar. In this study of older adults (and our previous study of young adults [6]), there were non-significant decreases in rightward angular momentum and average moment during right double support and left single support during pre-planned turns vs. straight-line gait. The decreased rightward angular momentum generation likely facilitates a net change in body facing direction leftward, though this non-significant observation warrants further investigation.

For context, we offer a description of balance measures and momenta control in other axes and initial exploration of gait speed. Left double support was the phase used to generate the most leftward transverse plane angular momentum during leftward turns. Left double support was also the phase with the largest average leftward force, though this trend was not significant at a group level. Additionally, in the frontal-plane, left double support was also when the distance between the lateral edge of the base of support and the COM is minimal (LD_{min}) and when the frontal-plane angular momentum reaches extrema such that the body above the COM rotates leftward ($H_{f,min}$) (Supplemental Document 3). Thus, left double support is a phase that may have specific balance control demands during turns. To meet these demands, the healthy older adults in this study also exhibited that their average frontal plane moment ($M_{f,avg}$) would tend to rotate the body in the opposite (rightward) direction during that phase; facilitating balance even if the frontal-plane balance measures are at extrema. In other words, even though the body can be tilting leftward ($H_f < 0$), the moment applied would tend to arrest this rotation ($M_{f,avg} > 0$).

The within-participant statistical analyses included in Supplemental Document 4 revealed that not all older adults in this cohort exhibited the group statistical findings. For example, one participant generated the greatest change in angular momentum during right single support during straight-line gait (participant 7 as seen in Figs. 2C and 4A). During straight line gait, two of nine did not follow the group trend for average leftward force being significantly greatest during right single support (participants 3 and 8; Fig. 3A). During turns, two of nine did not generate significantly greater linear momentum during right single support (participants 2 and 7; Fig. 2C) and two of nine did not generate statistically less average leftward force during left single support (participants 2 and 8; Fig. 3C). Interestingly, seven of nine participants demonstrated (not necessarily significantly) that the estimated marginal mean of the average leftward force was greatest during left double support during turns, with two of these participants exhibiting this trend significantly. This is interesting given the challenges to balance that may occur during left double support, such as minima in lateral distance and frontal-plane angular momentum (as discussed in the prior paragraph). The within-participant results in our prior study of young adults [6] indicated that only three of ten young adults exhibited the greatest estimated marginal means of the average leftward force occurring during left double support, with none exhibiting this trend significantly.

There are a few possible contributing factors for participant-specific responses that we propose to investigate in the future. For one, there is no mechanical *necessity* to generate greater linear momentum or average leftward forces during certain gait phases. Additionally, linear metrics (change in leftward momentum and average leftward force) may be moderated by turn strategy, as indicated by our preliminary exploration of this factor. Gait asymmetry in older adults [27, 28] may also contribute to momenta generation occurring in differing gait-phases. For example, during straight line gait, participants 3 and 8 generated approximately equal leftward force during right single support and left double support, rather than exhibiting greater leftward force during right single support (Fig. 3A). As another possible contributing factor, older adults have been found to use longer double support durations than young adults, especially if they are navigating around obstacles or fearful of falls [29, 30]. Our cohort of older adults used double support durations as a percent of gait cycle that were, on average, 33.47% (± 1.84% standard deviation) during straight-line gait and 34.16% (± 2.19% standard deviation) during turns. Thus, for some participants, the linear momentum that could otherwise be generated within the single support phase could become more distributed across single and double support phases. Future research can elucidate if momenta generation that is less distinct between gait-phases is observed more frequently in balance-impaired populations.

The detailed understanding of the momenta generation strategies used by healthy individuals during turns can be used to establish approaches for more targeted rehabilitation. For instance, let us imagine a future case of an individual receiving balance rehabilitation after falls that occur when circumventing obstacles. We find that during leftward turns, they generate the largest leftward linear and angular momenta during left single support—while also experiencing extrema in their frontal-plane balance metrics (e.g., angular momentum and LD minima) during left single support. This information allows pinpointing treatment to improve momenta control within specific stance configurations and dynamics. This momenta control intervention could include practicing generating leftward linear momentum during right single support contexts (e.g., side-stepping exercises initiated from right single support) and generating leftward angular momentum during left double support contexts (e.g., practicing axial rotations while in tandem stances of different widths). This intervention may also include de-coupling changes in body rotation and linear translation, strengthening left hip abductors, planning a wider turn radius or stepping strategies that reduce the likelihood of precarious balance states [20], practicing recovery steps after leftward perturbations, etc. The intervention outcome measure could include reaching targets for momenta generation for each gait phase using established healthy ranges for momenta control.

During turns, the older adults used a significantly slower gait speed than they used during straight-line gait (Supplemental Document 3) [6]. While future studies can better elucidate what happens during turns performed at different speeds, we initially explored accounting for gait speed statistically in this study (Supplemental

Document 2). The effect of gait phase on each of the four primary variables was not moderated by gait speed for any variable ($p \geq 0.09$). The older adults' slow gait speed yielded a COM trajectory in some participants visually similar to those illustrated by [8] during a 270° turn (with 1-m radius curved walkway) performed at gait speeds between 0.6 m/s and 1.0 m/s. The visual similarity included straighter COM trajectory portions interlaced with smaller curves, which stands in contrast to the smooth curvature of the COM trajectory we observed in young adults during pre-planned turns [6]. We postulate that this COM trajectory could be further studied with respect to older adults' reduced momenta control abilities, as they may be alternating between prioritizing changing direction (the curved portions) and balance maintenance (the straighter portions) across multiple footfalls.

This study has several limitations, primarily methodological. We have a small sample size of nine healthy older adults, who do not represent the general older adult population. They had not fallen in the past six months and were quite active: exercising often and walking five to ten hours per week (physical activity levels included in Supplemental Document 1). Next, by averaging across multiple instances of gait phases, we may be reporting attenuated momenta, acceleration, or moment generation for each gait phase. For example, in Fig. 1, the first right single support phase has significantly more change in linear momentum than does the second instance of right single support. As discussed, gait speed was not controlled, which allowed us to capture how individuals chose to navigate this turning task, closer to representing well-practiced real-world walking turns. However, future research can experimentally control gait speeds, which may minimize across-participant differences and build a better understanding of how momenta is controlled during faster and more challenging turns. Finally, we chose to examine momenta generation from a lab-fixed perspective to align with the global transverse-plane mechanical objectives of the turn. Naturally, this affects our interpretation of the data compared to a body-fixed reference frame, especially for the linear momenta metrics [31].

Future work related to momenta control during turns can focus on any of several areas to inform more specific clinical targets in rehabilitation. For instance, by better understanding the three-dimensional coordination of momenta control during turns with a larger and more gender-balanced sample, clinical indicators of balance dysfunction and normative targets can be further developed. It is also important to investigate direct comparisons between fall-prone and not fall-prone older adults, as well as other balance-impaired other populations. Future work may also benefit from understanding momenta control per gait phase from body-fixed reference frames or joint-level comparisons to inform clinical targets specific to segmental coordination and joint strength.

Conclusion

During 90° left turns, healthy older adults generated the greatest linear momentum in the direction of the turn (leftward in the global coordinate system) during right single support, and the greatest angular momentum in the direction of the turn (leftward in the transverse plane) during left double support. These findings are among the first descriptions of older adult momenta control during turns and provide a foundation for future work to improve older adults' preventative and rehabilitative care. Understanding momentum control within each phase of gait can help design more specific targets in gait and balance training interventions.

Abbreviations

ML	Medial–lateral
AP	Anterior–posterior
LD	Lateral distance
P	Whole-body linear momentum
Px	Linear momentum in the lab-fixed X direction
Py	Linear momentum in the lab-fixed Y direction
H	Whole-body angular momentum
Hf	Angular momentum in the pelvis-fixed frontal plane
Hz	Angular momentum in the transverse plane, about the vertical axis
Δp	Change in linear momentum
ΔH	Change in angular momentum
F_{avg}	Average force
M_{avg}	Average moment
$H_{f,min}$	Minimum frontal-plane angular momentum
LD_{min}	Minimum lateral distance
Δp_x	Change in linear momentum in the lab-fixed X direction
$F_{x,avg}$	Average force in the lab-fixed X direction
ΔH_z	Change in angular momentum in the transverse plane
$M_{z,avg}$	Average moment in the lab-fixed Z direction
LDS	Left double support
LSS	Left single support
RDS	Right double support
RSS	Right single support

Supplementary Information

The online version contains supplementary material available at https://doi.org/10.1186/s12984-024-01437-3.

Supplementary Material 1

Supplementary Material 2

Supplementary Material 3

Supplementary Material 4

Acknowledgements

We thank our research participants, the study Physical Therapist Alison Clark, and undergraduate research assistants Virina Botros and Sophia Donskoy for their assistance.

Author contributions

MT, ZH, JML collected the data. MT processed the data. MT and AZ interpreted the data. JM performed statistical analysis. MT wrote the first draft of the manuscript and edited drafts. AZ edited drafts, secured funding for the research, and finalized the manuscript for submission. All authors read and approved the final manuscript.

Funding

This study is funded by NSF Award #1944207. The funder did not have any role in the conceptualization, design, data collection, analysis, or publication process.

Availability of data and materials

All data generated or analyzed during this study are included in this published article and its supplementary information files.

Declarations

Ethics approval and consent to participate

Stevens Institute of Technology Institutional Review Board approved the study (IRB Protocol #: 2021-033) and participants provided written informed consent.

Consent for publication

Not applicable.

Competing interests

The authors declare no competing interests.

Received: 22 December 2023 Accepted: 2 August 2024
Published online: 23 August 2024

References

1. Herr H, Popovic M. Angular momentum in human walking. J Exp Biol. 2008;211:467–81.
2. Glaister BC, Bernatz GC, Klute GK, Orendurff MS. Video task analysis of turning during activities of daily living. Gait Posture. 2007;25:289–94.
3. Farrell MT, Herr H. Angular momentum primitives for human turning: control implications for biped robots. In: Proceedings of Humanoids 2008-8th IEEE-RAS International Conference on Humanoid Robots, Daejeon, Korea (South). 2008. p. 163–7.
4. Seidler RD, Bernard JA, Burutolu TB, Fling BW, Gordon MT, Gwin JT, et al. Motor control and aging: links to age-related brain structural, functional, and biochemical effects. Neurosci Biobehav Rev. 2010;34:721–33.
5. Bruijn SM, Van Dieën JH. Control of human gait stability through foot placement. J R Soc Interface. 2018;15:20170816.
6. Tillman M, Molino J, Zaferiou AM. Gait-phase specific transverse-plane momenta generation during pre-planned and late-cued 90 degree turns while walking. Sci Rep. 2023;13:6846.
7. Glaister BC, Orendurff MS, Schoen JA, Bernatz GC, Klute GK. Ground reaction forces and impulses during a transient turning maneuver. J Biomech. 2008;41:3090–3.
8. Orendurff MS, Segal AD, Berge JS, Flick KC, Spanier D, Klute GK. The kinematics and kinetics of turning: limb asymmetries associated with walking a circular path. Gait Posture. 2006;23:106–11.
9. Taylor MJD, Dabnichki P, Strike SC. A three-dimensional biomechanical comparison between turning strategies during the stance phase of walking. Hum Mov Sci. 2005;24:558–73.
10. Nolasco LA, Silverman AK, Gates DH. Whole-body and segment angular momentum during 90-degree turns. Gait Posture. 2019;70:12–9.
11. Nasreddine ZS, Phillips NA, Bedirian V, Charbonneau S, Whitehead V, Collin I, et al. The Montreal Cognitive Assessment, MoCA: a brief screening tool for mild cognitive impairment: MOCA: a brief screening tool for MCI. J Am Geriatr Soc. 2005;53:695–9.
12. Shumway-Cook A, Woollacott MH. Motor control: translating research into clinical practice. 4th ed. Philadelphia: Lippincott Williams & Wilkins; 2014.
13. Harrington ME, Zavatsky AB, Lawson SEM, Yuan Z, Theologis TN. Prediction of the hip joint centre in adults, children, and patients with cerebral palsy based on magnetic resonance imaging. J Biomech. 2007;40:595–602.
14. Rab G, Petuskey K, Bagley A. A method for determination of upper extremity kinematics. Gait Posture. 2002;15:113–9.
15. Dumas R, Chèze L, Verriest JP. Adjustments to McConville et al. and Young et al. body segment inertial parameters. J Biomech. 2007;40:543–53.
16. Fino PC, Lockhart TE, Fino NF. Corner height influences center of mass kinematics and path trajectory during turning. J Biomech. 2015;48:104–12.
17. Department of Justice. 2010 ADA Standards for Accessible Design. USA; 2010. https://www.ada.gov/regs2010/2010ADAStandards/2010ADAStandards.htm. Accessed on 7 Aug 2024.
18. Kumar S, Fernando DJS, Veves A, Knowles EA, Young MJ, Boulton AJM. Semmes-Weinstein monofilaments: a simple, effective and inexpensive screening device for identifying diabetic patients at risk of foot ulceration. Diabetes Res Clin Pract. 1991;13:63–7.
19. Potter K, Brandfass K. The mini-balance evaluation systems test (Mini-BESTest). J Physiother. 2015;61:225.
20. Tillman M, Molino J, Zaferiou AM. Frontal plane balance during pre-planned and late-cued 90 degree turns while walking. J Biomech. 2022;141:111206.
21. Zeni JA, Richards JG, Higginson JS. Two simple methods for determining gait events during treadmill and overground walking using kinematic data. Gait Posture. 2008;27:710–4.
22. Ulrich B, Santos AN, Jolles BM, Benninger DH, Favre J. Gait events during turning can be detected using kinematic features originally proposed for the analysis of straight-line walking. J Biomech. 2019;91:69–78.
23. Golyski PR, Hendershot BD. A computational algorithm for classifying step and spin turns using pelvic center of mass trajectory and foot position. J Biomech. 2017;54:96–100.
24. Hase K, Stein RB. Turning strategies during human walking. J Neurophysiol. 1999;81:2914–22.
25. Leestma JK, Golyski PR, Smith CR, Sawicki GS, Young AJ. Linking whole-body angular momentum and step placement during perturbed walking. J Exp Biol. 2023;226: jeb.244760.
26. Zaferiou AM, Wilcox RR, McNitt-Gray JL. Modification of impulse generation during pirouette turns with increased rotational demands. J Appl Biomech. 2016;32:425–32.
27. Yogev G, Plotnik M, Peretz C, et al. Gait asymmetry in patients with Parkinson's disease and elderly fallers: when does the bilateral coordination of gait require attention? Exp Brain Res. 2007;177:336–46. https://doi.org/10.1007/s00221-006-0676-3.
28. Laroche DP, Cook SB, Mackala K. Strength asymmetry increases gait asymmetry and variability in older women. Med Sci Sports Exerc. 2012;44(11):2172–81. https://doi.org/10.1249/MSS.0b013e31825e1d31.
29. Caetano MJD, Lord SR, Schoene D, Pelicioni PHS, Sturnieks DL, Menant JC. Age-related changes in gait adaptability in response to unpredictable obstacles and stepping targets. Gait Posture. 2016;46:35–41.
30. Maki BE. Gait changes in older adults: predictors of falls or indicators of fear? J Am Geriatr Soc. 1997;45:313–20.
31. Glaister BC, Orendurff MS, Schoen JA, Klute GK. Rotating horizontal ground reaction forces to the body path of progression. J Biomech. 2007;40:3527–32.

Publisher's Note